Whole Life-cycle of Superfilament in Water
From Femtoseconds up to Microseconds

F. V. Potemkin, E. I. Mareev, A. A. Podshivalov and V. M. Gordienko
Faculty of Physics and International Laser Center M.V. Lomonosov Moscow State University, Moscow, Russia

Keywords: Femtosecond Superfilament, Laser-induced Shock Waves, Laser-induced Cavitation, Aberrations, Linear Absorption.

Abstract: A whole life-cycle of the superfilamentation in water in tight focusing geometry was investigated. In this regime a single continuous plasma channel is formed. To achieve this specific regime the principal requirement is the usage of tight focusing and supercritical power of laser radiation. They together clamp the energy in the ultra-thin (approximately several microns) channel with a uniform plasma density distribution in it. The superfilament becomes a center of cylindrical cavitation bubble area and shock wave formation. The length of the filament increases logarithmically with laser pulse energy. The linear absorption decreases the incoming energy delivered to the focal spot, which dramatically complicates the filament formation, especially in the case of loose focusing. Aberrations added to the optical scheme lead to multiple dotted plasma sources for shock wave formation, spaced along the axis of pulse propagation. Increasing the laser energy launches the filaments at each of the dot, whose overlapping leads to enhance the length of the whole filament.

1 INTRODUCTION

When a femtosecond laser pulse is tightly focused inside the water cell, extreme for the medium intensities ($I \sim 10^{13}$ W/cm^2) are achieved in the focal region, and electron plasma is generated (Potemkin et al. 2014). The high temperatures ($T_e \sim 10$eV), achieved in the laser plasma lead to a thin layer of water vapor generation. The layer begins to expand with a supersonic speed, than emits a shock wave and at last forms a cavitation bubble. After separation from the layer, shock wave begins propagation through the medium until it dying. The cavitation bubble comes over several oscillations until it collapse. Because the energy is transmitted from the plasma to the medium through electron-ion collisions, initially the cavitation bubble and the shock front shape replicates the shape of the laser-induced plasma (Lauterborn & Vogel 2013). Thus, the shock wave profile replicates the initial pressure distribution in plasma, and therefore in order to control the shock wave shape, one must take care of the distribution of the energy conserved in the plasma (Noack and Vogel 1999). The processes, which could affect on the initial plasma density and intensity distribution dramatically changes the evolution of the superfilament and its post-effects. In the work we investigate the role of focusing regimes, laser parameters and medium properties (linear absorption) in the process of ultra-short laser pulse superfilamentation in water as the most convenient prototype of condensed medium. This work is a pioneering attempt to investigate the superfilament and its post-effects in water under tight focusing geometry. Additionally for the first time we found out the unique experimental conditions demonstrated controllable reversible transition from the regime of multiple filamentation to superfilamentation in condensed matter

2 EXPERIMENTAL SETUP

In the experiments, a Cr:forsterite femtosecond laser (wavelength of 1240 nm, pulse duration about 140 fs, laser energy up to 150 μJ, intensity contrast about 5×10^9 ASE, and repetition rate of 10Hz) was employed. Shadow photography technique was applied for probing the dynamics of laser-induced shock waves and cavitation bubbles. In this technique, the probe pulse (used as a strobe) passes through the sample and creates a uniform

Potemkin F., Mareev E., Podshivalov A. and Gordienko V..
Whole Life-cycle of Superfilament in Water - From Femtoseconds up to Microseconds.
DOI: 10.5220/0005403801220127
In *Proceedings of the 3rd International Conference on Photonics, Optics and Laser Technology* (PHOTOPTICS-2015), pages 122-127
ISBN: 978-989-758-093-2

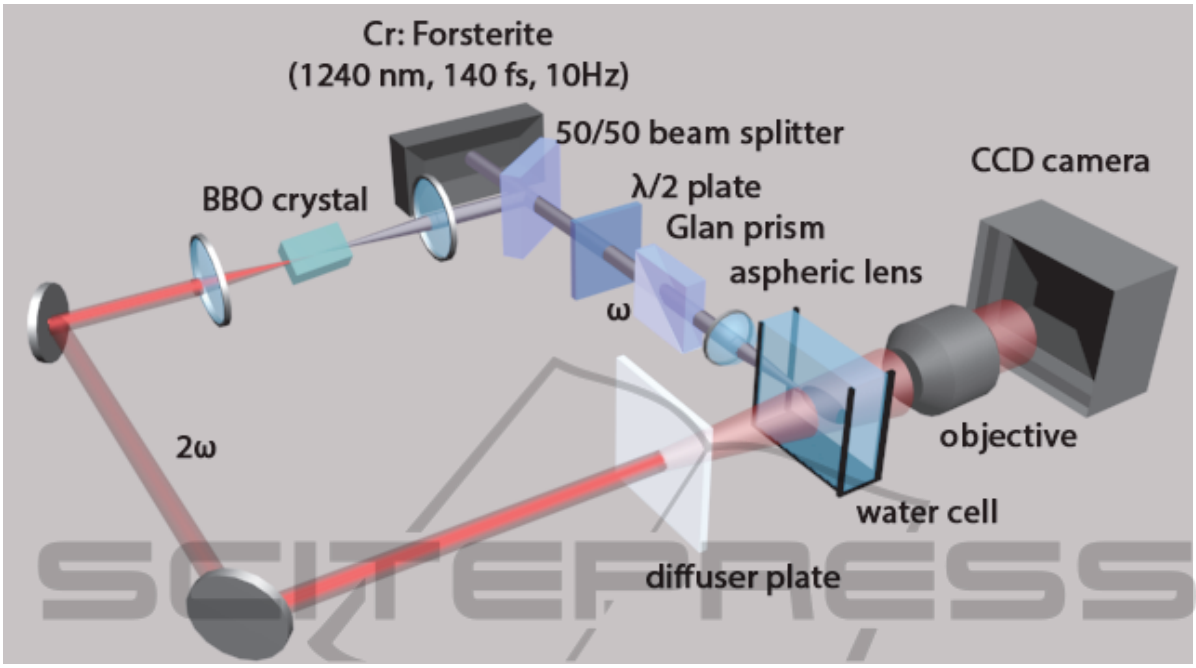

Figure 1: Experimental setup. The incoming femtosecond laser pulse splits into two channels. The pump pulse is tightly focused by an aspheric lens into the water cell. The energy of the pump pulse is varied by half-wave plate and Glan prism. The second harmonic is used as a probe pulse. It is scattered in a ground glass plate. Passing through the water cell with a shock wave, the probe radiation is collected by the microscopic objective on the CCD matrix. Temporal resolution of this scheme is about 200 fs; optical delay can be changed with adjusting mirror position from zero to 25 nanoseconds.

illumination on a CCD camera. The perturbations in the refractive index, induced by the pressure waves, act as scattering centers and are seen as dark areas on the CCD matrix. The experimental scheme is sketched in Fig.1. The beam splitter divided the initial laser beam into two beams: pump and probe. The half-wave plate with Glan prism was used for attenuation of the incident pulse energy. In the incident wavelength, water strongly absorbs laser radiation due to resonance with molecular vibrations, which lead to significant linear absorption.

Therefore, taking into account linear absorption of water at 1240 nm about 0.9 cm^{-1} only 74% (3.3mm focusing lens) and 69% (4.6mm focusing lens) of incoming energy was delivered to the focal waist. Tight focusing of the laser beam into the water cell leads to the strong spherical aberrations. Placing the focusing lens inside the water cell allowed us to minimize these aberrations.

3 RESULTS AND DISCUSSION

Filamentation usually defines, as a dynamical balance among self-focusing, plasma defocussing and diffraction, when supercritical laser radiation propagates through a nonlinear medium (Couairon and Mysyrowicz 2007). On the one hand, the optical Kerr effect acts against diffraction and tends to focus the beam on itself. On the other hand, multiphoton absorption limits the intensity, because the laser-induced plasma acts as a defocusing center. Usually filamentation is accompanied by the conic emission and strong luminescence from multiple "filaments"(Couairon and Mysyrowicz 2007). In a normal wisdom, in a tight focusing regime (NA>0.3) the diffraction sufficiently overcomes the Kerr self-focusing just after the focal spot, therefore the filament can`t be fired. The formation of laser-induced shock waves and cavitation bubbles inside the condensed medium is a threshold effect: shock waves are formed, when the electron density is high enough (~10^{19} cm^{-3}) and the cavitation bubbles are formed, when the electron density is about 10^{18} cm^{-3} (Vogel et al., 2008). When laser radiation was focused by 3.3mm focusing lens, threshold of shock wave formation could be measured at 4±0.5μJ (laser intensity is about 10^{13} W/cm^2). The energy stored in shock waves and cavitation bubbles and, therefore, amplitude and speed of shock waves and the diameter ($E \sim D^3$) of cavitation bubbles strongly depend on the electron concentration. Thus, they are

perfect tools for probing the plasma density distribution.

3.1 Role of the Focusing Geometry in the Filament Formation

The first series of the experiments were carried out with comparatively loose focusing (NA=0.1). This close to classical regime enables a bright conical emission and multifilamentation.

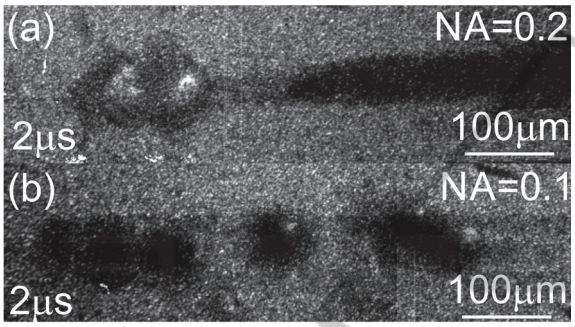

Figure 2: The cavitation bubble pattern induced by the laser filament in water (laser pulse energy 190±10μJ, time delay 2μs). (a) There is a plasma channel in the right part of the picture, which transforms into several randomly distributed cavitation bubbles. No visible luminescence or conical emission is observed (b) There are multiple randomly distributed cavitation bubbles, but there is no plasma channel. In this case the visible luminescence from the filament and conical emission were observed.

Only at high (about 40 P_{cr}) power of the laser beam the multiple filaments could be visually observed, due to the high linear absorption, which sufficiently complicate the process of filament formation. The intensity clamping limits the electron density, which is not exceeding $3x10^{18}$ cm^{-3}(Minardi et al., 2008). Therefore, loose focusing of a laser beam cannot achieve high electron densities due to the intensity clamping in the filament, and additionally, the breaking of one filament into multiple filaments diffuses the laser energy over a huge area. In these conditions no shock waves are formed, because there is not enough energy localization characterized by electron density (Vogel et al., 2008). In this case, the shadow photographs show no shock wave formation. However, if we increase the laser energy (in this case the time delay is varied electronically by the delay generator), a random distribution of cavitation bubbles can be observed (Fig.2). The energy distribution along the filament axis is stochastic and a significant amount of energy is deliver to the non-linear Kerr foci. These Kerr foci become centres of the cavitation bubble formation. Thus, the radii and position of the bubbles change from pulse to pulse, because the energy issued in each focus determines the diameter of each bubble ($E \sim D^3$).

The opposite case is tight focusing (NA>0.3) of the laser beam (Fig.3). In this regime the shadow pictures show plasma channels much longer than the Rayleigh length. Now let us discuss in detail the physical processes that take place under tight focusing of intense laser radiation into fresh water. The intensity in condensed matter is strongly limited by the nonlinear absorption (Mikheev and Potemkin 2011). In the case of tight focusing, the laser intensity in the focal spot can reach values up to 10^{14} W/cm^2 this is an upper limit of a rough estimate; such experimental values were estimated based on the CE broadening in filament under tight focusing in water (Couairon and Mysyrowicz 2007). Therefore the electron density is about $0.1n_{cr}$ ($n_{cr}=m_e\omega^2/4\pi e^2 \cong 7.3\times10^{20} cm^{-3}$) and the plasma electron energy is sufficiently larger than in loosely focusing geometry. In this regime the energy is localized in the microvolume with 4 μm in diameter, and multiple filaments interact with each other and a single continuous filament is created (Point et al., 2014). To determine the contribution of different processes (plasma defocusing, Kerr self-focusing and diffraction), simple estimates can be made. The length of self-focusing can be estimated as $L_{sf}=\lambda/2\pi n_2 I \approx 800nm$ ($n_2=1{,}6\times10^{-16}$ cm^2/W), the length scale for plasma defocusing $L_{defoc}=L_{pl}n_{at}/n_e=n_0\lambda n_{cr}/\pi n_e \approx 5\mu m$, and the diffraction length is a Rayleigh length which is about 15 μm. Therefore, the Kerr self-focusing does not allow the laser radiation to leave the optical axis, and one continuous filament with approximately uniform distribution of electron concentration along the optical axis can be formed. This can be confirmed by the fact that the radius of the shock wave and cavitation bubble is uniform along the filament axis, and its radius strongly depends on the plasma electrons' mean energy and density. The shape and the size of the cavitation area and shock waves do not change from pulse to pulse. To simplify, when the laser beam is tightly focused into the bulk of the condensed matter, it cannot deliver all the energy to one point and then transmit energy further until it will be absorbed. The nonlinear processes limit intensity in each point of such a channel, as will be shown in the text. With the energy increase the electron concentration is limited in the channel (Fig.3a), but the length of the filament continues its growth (see Fig.3d). Therefore, the superfilament continues its life on the femtosecond time-scale.

For 0.2<NA<0.3 the energy localization on the

optical axis grew, and competition with strong energy exchange between different filaments occurred. This led to random filament distribution across the laser beam, and each filament launched a shock wave, but in sum they do not form one contrast wave (Abraham et al., 2000). Nonetheless, laser-induced cavitation bubbles can be a better indicator for filament characterization. Initially, the array of laser-induced cavitation bubbles form one cylindrical cavitation area (Fig.2a), as in the case of tighter focusing. But after an approximate 1mm distance, the superfilament breaks into multiple filaments and multiple bubble formation can be observed. These multiple bubbles, as in the case of loose focusing, are randomly disturbed.

3.2 Role of Linear Absorption

Cr:Forsterite laser wavelength (1240nm) falls in the absorption band of water molecules vibrations cantered at 1200nm, which leads to a high linear absorption (about 0.9cm^{-1}); such high absorption strongly violates the processes of filament formation and further shock wave and cavitation bubble generation. To identify the role of the linear absorption, additional experiments were carried out with heavy water (D_2O). Heavy water has similar physical properties to water, but the vibrational frequencies are different. The fact allowed us to avoid resonant interaction between the laser radiation and water molecules.

The amount of the absorbed energy is proportional to the distance travelled by the laser beam inside the water. Therefore, to achieve high intensities in the focal spot, it is necessary to use lenses with small focusing distance or alternately focus the radiation near the water boundary. The most significant role the absorption of the laser energy will play in the case of loose focusing. When the laser radiation was focused into a cell with D_20, the visibility of the filament and the number and size of the cavitation bubbles (the volume of the cavitation area determines the energy delivery to the medium) was greater than in the case of H_20.

In the case of tight focusing into the water cell, the nonlinear absorption starts to play the main role and the difference between the D_2O and H_2O becomes less significant. To compare the length of the plasma channels it is easy to use the cavitation bubble area. The experiments show that with a decrease of focusing distance, the length of the plasma channel grows.

3.3 The Evolution of Filament-induced Shock Wave

Now let us concentrate on the filament-induced shock wave evolution, taking place on the nanosecond timescale. The shadow photographs, provided in Fig.3(a-c), show that instead of a spherical shock wave, the cylindrical shock wave was generated, because the each point of the superfilament becomes a centre of spherical shock waves and cavitation bubble formation.

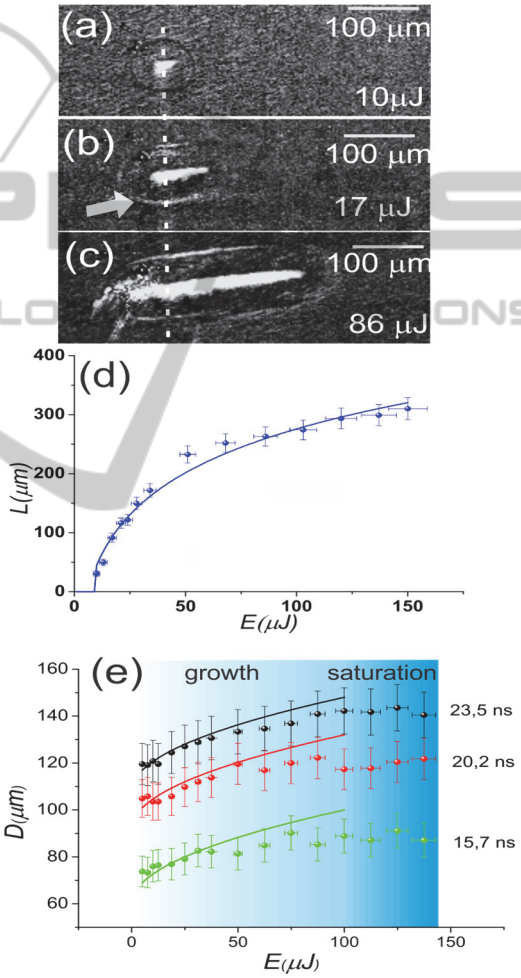

Figure 3: (a-c) The shadow pictures of the filament-induced shock waves (time delay 15ns, NA=0.4, f=3.3mm) at different energies, (d) the length of the filament on the laser pulse energy, (e) the diameter of the shock wave on the laser pulse energy.

At energies just above the threshold, one spherical shock wave was formed (Fig.3a). With the increase of laser energy a single, stable (from pulse to pulse), cylindrical shock wave was generated. As was discussed above, the shock waves were generated

only in the areas where the electron density was greater than the threshold. The amplitude and the initial speed of the shock wave were fully described by the initial pressure distribution inside the laser-induced plasma. In our case, the extreme intensity in the focal spot leads to a stable continuous superfilament formation. Initially the cavitation region in the centre of the picture replicates the shape of the filament, and therefore the length of the filament can also be restored from the pictures; the errors of such rough estimates do not exceed the diameter of each cavitation bubble. The filament length has a logarithmic dependence on laser pulse energy (Fig.3d). The pressure on the front of the shock wave can be restored from the shock wave speed using the semi-empirical equation $p_s = c_1 \rho_0 u_s (10^{(u_s - c_0)/c_2} - 1)$. Here c_1,c_2 are empirical constants, c_0 is the speed of sound in the medium, ρ_0 is the density of the undisturbed medium, and us is the speed of the shock wave front. In water c_0 = 1483 m/s, ρ_0 = 998 kg/m^3, c_1 = 5190 m/s and c_2 = 25 306 m/s. Thus assuming the exponential decay of the shock wave speed, we can calculate the shock wave speed. For incident laser energy of 130μJ, shock wave front velocity is 2300±200m/s. The shock pressure can be estimated as 1.0±0.1 GPa.

We performed another series of experiments to investigate the dynamics of filament-induced shock waves on the laser pulse energy. The results are shown in Fig.3e. We found, that shock wave diameter tends toward saturation as a square root of incident pulse energy. The saturation of the shock wave energy (which is proportional to its speed), is caused by the intensity clamping. With the increase of the laser pulse energy the plasma electron density tends toward saturation, due to a limitation of electrons in the effected volume (Mikheev & Potemkin 2011). Thus the energy, that can be transferred from laser radiation to plasma and then from plasma to each shock wave in the optical breakdown volume, is limited. Nevertheless, the length of the filament continues to increase, because there is still enough energy in the energy reservoir. Thus, varying only the energy of laser pulse shape, we can change the spatial characteristics of the laser-induced shock wave.

3.4 Role of Aberrations

The last way to control the shock wave shape is using the aberrations. The aberrations often limit the possibilities of laser beam tight focusing inside the medium. Briefly, when the laser beam tightly focuses into the bulk of the medium, the convergence angles are big; due to the Snell`s law the different rays are focused in different points of the medium, leading to significant spherical aberrations. A more complicated theory of the process can be found in (Marcinkevičius et al. 2003). In our case the most important result is formation of intensity maxima along the optical axis, which becomes the centres of filament generation.

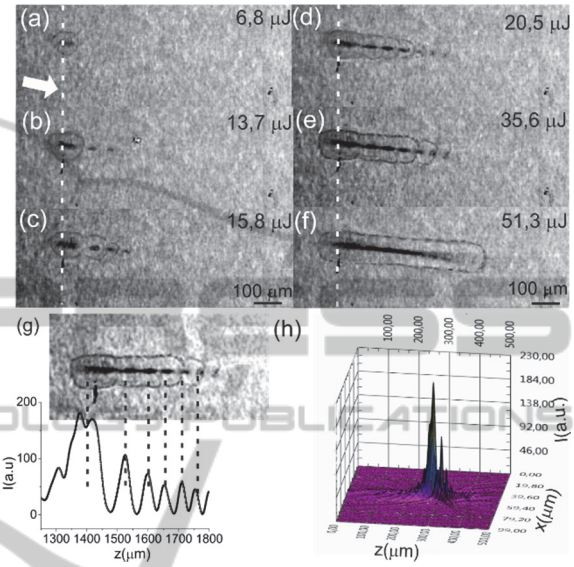

Figure 4: The evolution of the shock waves and cavitation bubbles on the laser pulse energy with aberrations. (a)-(f) shadowgrams of shock waves and cavitation bubbles, delayed on 18.6 ns from optical breakdown at different incident laser pulse energy: (a) 6.8, (b) 13.7, (c) 15.8, (d) 20.5, (e) 35.6 and (f) 51.3 μJ. The laser radiation was focused by the 4.6mm focusing lens (NA=0.3). (g,h) The numerical calculation of the intensity profiles after focusing of the laser beam into water for NA=0.3, d=1,3mm and the shadow picture of the corresponding laser-induced shock waves and cavitation bubbles.

In this regime, complex spatial patterns of shock waves can be generated. The intensity profile maxima become the centres for cavitation bubble and spherical shock wave generation. At low laser pulse energy only single spherical shock waves are generated (Fig. 4a), while at higher laser pulse energy several dotted sources, isolated from each other, create a complex envelope of shock wave (Fig. 4c-e). With the increase of laser energy additional shock waves are generated from new plasma, forming a cylindrical shock wave (Fig. 4f). Such aberrations could effectively increase the length of the laser filament and the laser-induced shock impact on the material.

4 CONCLUSIONS

In conclusion, we investigated the whole life (from femtoseconds to microseconds) of the superfilament, fired in water under a supercritical power regime from the laser pulse energy, focusing and linear absorption. The high intensity clamps the energy into a thin layer along the filament axis. It leads to the channel formation with extreme and quasi-uniform electron density distribution. The increase of the laser pulse energy does not change plasma density but sufficiently enlarges the superfilament length. The superfilament became a centre of cylindrical cavitation area formation and shock wave generation. The maximal velocities and pressures achieved for the incident laser energy of 130μJ on the shock wave front were 2300±200m/s and 1.0±0.1 GPa, respectively. The length of the filament was logarithmically dependent on laser pulse energy. The diameter of the filament grew as a square root of laser pulse energy and tended toward saturation, which was caused by the saturation of plasma electrons' density. When the looser (NA<0.1) focusing was employed there was no continuous plasma channel and shock wave generation, but instead a conical emission and randomly-generated cavitation bubbles were observed, as the energy delivered to the medium by plasma electrons was not high enough for contrast shock wave generation. In the case of medium focusing (0.1<NA<0.3) the superfilament, once created close to the water-air boundary, breaks up into a randomly distributed pattern of cavitation bubbles. The linear absorption significantly increased the threshold of filament ignition due to the effective laser energy transferring to the vibrational modes of H_2O molecules. Aberrations added to the optical scheme led to multiple dotted plasma sources for shock wave formation, spaced along the axis of pulse propagation. Increasing the laser energy launches the filaments at each of the dot, whose overlapping provides to enhance the length of the whole filament and resulted in growth of shock impact on the material.

ACKNOWLEDGEMENTS

This research has been supported by the Russian Foundation for Basic Research (Projects No. 14-02-00819a and No. 14-29-0723) and partly by the M.V. Lomonosov Moscow State University Program of Development.

REFERENCES

Abraham, E., Minoshima, K. & Matsumoto, H., 2000. Femtosecond laser-induced breakdown in water : time-resolved shadow imaging and two-color interferometric imaging. *Optics and Spectroscopy*, 176, pp.441–452.

Couairon, A. & Mysyrowicz, A., 2007. Femtosecond filamentation in transparent media. *Physics Reports*, 441(2-4), pp.47–189.

Lauterborn, W. & Vogel, A., 2013. *Bubble Dynamics and Shock Waves* C. F. Delale, ed., Berlin, Heidelberg: Springer Berlin Heidelberg.

Marcinkevičius, a. et al., 2003. Effect of refractive index-mismatch on laser microfabrication in silica glass. *Applied Physics A: Materials Science & Processing*, 76(2), pp.257–260.

Mikheev, P.M. & Potemkin, F. V., 2011. Generation of the third harmonic of near IR femtosecond laser radiation tightly focused into the bulk of a transparent dielectric in the regime of plasma formation. *Moscow University Physics Bulletin*, 66(1), pp.19–24.

Minardi, S. et al., 2008. Time-resolved refractive index and absorption mapping of light-plasma filaments in water. *Optics letters*, 33(1), pp.86–8.

Noack, J. & Vogel, a., 1999. Laser-induced plasma formation in water at nanosecond to femtosecond time scales: calculation of thresholds, absorption coefficients, and energy density. *IEEE Journal of Quantum Electronics*, 35(8), pp.1156–1167.

Point, G. et al., 2014. Superfilamentation in Air. *Physical Review Letters*, 112(22), p.223902.

Potemkin, F. V et al., 2014. Laser control of filament-induced shock wave in water. *Laser Physics Letters*, 11(10), p.106001.

Vogel, A. et al., 2008. Femtosecond-Laser-Induced Nanocavitation in Water: Implications for Optical Breakdown Threshold and Cell Surgery. *Physical Review Letters*, 100(3), p.038102.